Experimental and numerical analyses of different extended surfaces

2012 J. Phys.: Conf. Ser. 395 012045

(http://iopscience.iop.org/1742-6596/395/1/012045)

Experimental and numerical analyses of different extended surfaces

A Diani[1], S Mancin[1,2], C Zilio[1] and L Rossetto[1]

[1]Dipartimento di Ingegneria Industriale, Università di Padova, via Venezia 1, 35131, Padova, Italy

Abstract. Air is a cheap and safe fluid, widely used in electronic, aerospace and air conditioning applications. Because of its poor heat transfer properties, it always flows through extended surfaces, such as finned surfaces, to enhance the convective heat transfer. In this paper, experimental results are reviewed and numerical studies during air forced convection through extended surfaces are presented. The thermal and hydraulic behaviours of a reference trapezoidal finned surface, experimentally evaluated by present authors in an open-circuit wind tunnel, has been compared with numerical simulations carried out by using the commercial CFD software COMSOL Multiphysics. Once the model has been validated, numerical simulations have been extended to other rectangular finned configurations, in order to study the effects of the fin thickness, fin pitch and fin height on the thermo-hydraulic behaviour of the extended surfaces. Moreover, several pin fin surfaces have been simulated in the same range of operating conditions previously analyzed. Numerical results about heat transfer and pressure drop, for both plain finned and pin fin surfaces, have been compared with empirical correlations from the open literature, and more accurate equations have been developed, proposed, and validated.

1. Introduction

Microelectronics devices, which include a variety of applications such as PCs, servers, laser diodes, aerospace crafts are constantly pushing the heat transfer flux density requirements to higher levels [1]. Efficient heat spreaders and dissipaters, and compact heat exchangers are of great demand for various applications. Considering the working fluid for electronic applications, high dielectric constant is needed, so up today, the only viable options as an alternative to air cooling are liquid or two-phase cooling with boiling FC or HFC.

Air represents the most safe and cheap natural working fluid for thermal management applications. Many technologies such as plain and louvered fins, pin fins, offset strip fins and wire screens have been developed and studied both analytically and experimentally in the past decades to increase the heat transfer area density of heat sinks without losing the necessary compactness. Due to their simplicity and reliability, finned surfaces are the most commonly used to cool electronic equipments. With the available modern numerical techniques, simulations are widely used to design and characterize new heat sinks, without the necessity of experimental set up and, thus, with relative lower costs. CFD models are a useful tool to predict heat transfer and fluid flow performance of heat sinks

[2] Corresponding author. E-mail: simone.mancin@unipd.it

and heat exchangers: once the numerical results have been validated with the experimental ones, an optimization design can lead to the best geometrical configuration.

This paper presents a numerical study of different rectangular finned surfaces, which have constant width and length, but different number of fins, fin thickness, and fin height. Three air inlet velocities (5, 7.5 and 10 m s^{-1}) have been analyzed. The model is validated with experimental values of heat transfer coefficient and pressure drop of a reference trapezoidal finned surface. Furthermore, the numerical tool has been used to simulate the heat transfer and fluid flow behavior of different pin fin surfaces. The numerical results of heat transfer and pressure drop have been compared with empirical correlations from the open literature, and four new equations for the prediction of heat transfer coefficients and pressure drops have been developed and here suggested.

2. Problem description

2.1 Reference finned surface

The reference finned surface, made of aluminum, presents six trapezoidal fins attached on a rectangular base of 70 X 100 X 12 mm^3. Each fin has a base width of 5 mm, a top width of 3 mm and it is 48 mm high. This enhanced surface has been previously tested by present authors in an experimental set up built at the Dipartimento di Ingegneria Industriale of the Università di Padova.

This test rig is an open-circuit type wind tunnel with a rectangular cross section and it has been designed and developed to study the heat transfer and fluid flow during air forced convection through several different enhanced surfaces, such as finned surfaces, offset strip fins, cellular structure materials both stochastic and periodic. A detailed description of the test rig is available in Mancin et al. [2-3]. The experiments have been conducted by varying the air mass flow rate from 0.010 kg s^{-1} to 0.026 kg s^{-1}, and two different heat fluxes have been investigated: 21.4 kW m^{-2} and 25.0 kW m^{-2}.

2.2 Numerical model

The baseline aluminum heat sinks, which are a rectangular finned extended surface and a pin fin surface, attached to a 2.5 mm base plate, are shown in figure 1, where w indicates the width of the finned surface, l the length of the sample, b the base plate height, H the height of the fins, p the fin pitch, t the fin thickness, S the longitudinal pin pitch and T the transversal pin pitch. All the simulated plain fin surfaces are characterized by the same overall dimensions, which are 100 mm in width and 100 mm in length, whereas the pin fin surfaces have the same number of pins (30) both in the stream-wise and in the span-wise direction: according to Short et al. [4-5], this arrangement guarantees a fully development of the flow in all the pin fin surface configurations.

Due to their symmetry, only a single channel of the finned surfaces has been simulated. The fluid domain (air with constant hydraulic and thermal properties) starts 50 mm before the solid domain (finned surface) and ends 50 mm after the solid domain. A sensitivity analysis of the effects of inlet and outlet ducts has been performed finding that 50 mm was the minimum length which does not affect the air velocity fields in the simulated range of the operating conditions.

Figure 1 also shows the view of the simulated domains; for the fluid-dynamic analysis, the boundary conditions are:

- symmetry on the lateral sides of both the solid domain and fluid domain;
- constant longitudinal velocity u_y at the inlet of the fluid domain ($u_x = u_z = 0$);
- no slip conditions at the wall interface between the solid and the fluid domain, at the top of the fluid domain and at the bottom of the inlet and outlet fluid domain;

for the thermal analysis, the boundary conditions are:

- symmetry on the lateral sides of both the solid domain and the fluid domain;
- temperature at the inlet of the fluid domain (25 °C);
- heat flux at the bottom of the solid domain (domain base) (25 kW m^{-2});
- adiabatic conditions at the top of the solid domain (top of the fins);
- adiabatic conditions at the top and at the bottom of the fluid domain.

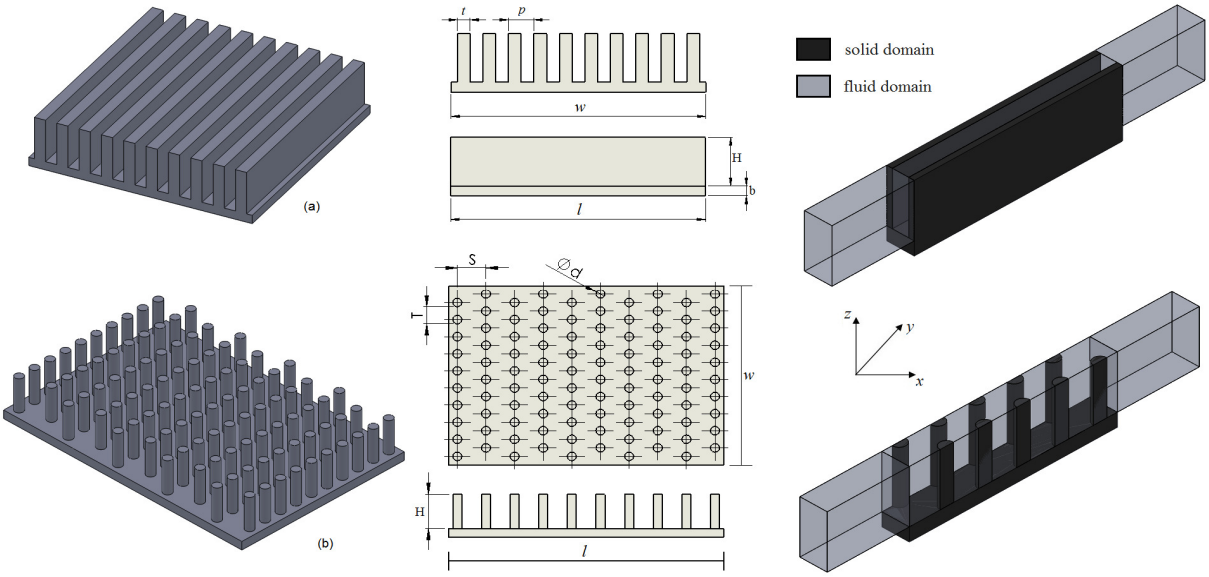

Figure 1. Geometries, dimensions and simulated channels: (a) plain fin and (b) pin fin heat sink.

A sensitivity analysis of the mesh has been carried out in order to avoid any mesh dependent results. Meshes are made up of tetrahedral elements. The number of the mesh elements for the plain fin surfaces ranges between 170000 and 300000, while for the pin fin surfaces between 280000 and 400000.

Conjugate problems, which included turbulent flow and heat transfer in air stream and heat conduction in the fins and in the base plate, were solved by using the commercial software COMSOL Multiphysics [6]. The velocity field has been simulated with the standard *k*-ε turbulence model.

2.3 Data reduction

For both the experimental and numerical data points, the heat balance between the imposed heat flux at the base of the sample and the air side heat flow rate has to be verified:

$$P_{EL} = \dot{m}_{AIR} \cdot c_{p,AIR} \cdot (t_{AIR,OUT} - t_{AIR,IN}) \tag{1}$$

where P_{EL} is the heat flow rate calculated from the constant value of the heat flux, 25 kW m^{-2}, $\dot{m}_{AIR}$ is the air mass flow rate, $c_{p,AIR}$ is the air mean specific heat capacity at constant pressure, $t_{AIR,OUT}$ and $t_{AIR,IN}$ are the outlet and inlet air temperatures, respectively. For the experimental results, the difference between the two terms of equation (1) was always lower than ±5%. Considering the numerical results, this difference was always lower than ±1%.

The product between the heat transfer coefficient α and the finned surface efficiency Ω^*, termed overall heat transfer coefficient α^*, is defined as:

$$\alpha^* = \alpha \cdot \Omega^* = \frac{P_{EL}}{A_{TOT} \cdot \Delta t_{ml}} \tag{2}$$

where A_{TOT} is the total heat transfer area of the finned surface and Δt_{ml} is the logarithmic mean temperature difference between the air and the surface:

$$\Delta t_{ml} = \frac{(t_{W,OUT} - t_{AIR,OUT}) - (t_{W,IN} - t_{AIR,IN})}{\ln \dfrac{t_{W,OUT} - t_{AIR,OUT}}{t_{W,IN} - t_{AIR,IN}}} \tag{3}$$

where $t_{W,OUT}$ and $t_{W,IN}$ are the temperatures of the base of the specimen at the outlet and at the inlet section, respectively.

According to the fin theory [7], the finned surface efficiency Ω^* can be calculated as:

$$\Omega^* = 1 - \frac{A_a}{A_{TOT}} \cdot (1 - \Omega) \tag{4}$$

where A_a is the fin surface area and Ω the fin efficiency, which, assuming adiabatic conditions at the top of the fins, can be expressed as:

$$\Omega = \frac{\tanh(m \cdot H)}{m \cdot H} \tag{5}$$

with:

for plain fin surfaces $$m = \sqrt{\frac{2 \cdot \alpha}{\lambda \cdot t}} \tag{6}$$

and for pin fin surfaces $$m = \sqrt{\frac{4 \cdot \alpha}{\lambda \cdot d}} \tag{7}$$

The finned surface efficiency Ω^* and the heat transfer coefficient α can be calculated from iterative procedure as presented by equations (2-7).

2.4 Model validation

The numerical model has been validated with the experimental heat transfer and pressure drop values obtained during experiments carried out on the reference trapezoidal finned surface [8]. The finned surface has been modelled as a solid body with a constant thermal conductivity λ of 175 W m^{-1} K^{-1}, whereas the fluid domain consists of air with constant thermal and hydraulic properties, such as density, viscosity, thermal conductivity and specific heat capacity at constant pressure, calculated at the mean values of temperature and pressure.

The numerical results are in good agreement with the experimental measurements [9]; in particular, the numerical ones tend to slightly underestimate the experimental values with a relative deviation of -3.4% and a standard deviation of 1.7%. Furthermore, the hydraulic numerical results show a good agreement for experimental pressure drops higher than 20 Pa, with a deviation lower than 4 Pa. At lower pressure drop, the deviation is lower than 2 Pa and the predictions worsen: this might be due also to the low accuracy of the experimental measurements in these working conditions. The relative deviation between the experimental and numerical pressure drop results is -3.6%, the absolute deviation 7.1% and the standard deviation 8.1%.

Globally, the numerical results show good agreement with the experimental ones, confirming the suitability of the simulation tool to predict the thermal and fluid dynamic behavior of finned surfaces.

3. Enhanced surface simulations

Starting from the comparison between the experimental and numerical results for the reference finned surface, the simulation tool has been used to predict the heat transfer performance of different plain finned and pin fin surfaces. For the plain finned surfaces, the number of fins has been varied between 9 and 15, the fin thickness from 2 to 6 mm and the fin height from 10 to 20 mm; the fin pitch is calculated as the ratio between the width of the heat sink and the number of fins; in these geometrical ranges, the ratio t/H varies between 0.1 and 0.6, whereas the ratio p/H between 0.33 and 1.11. For the pin fin heat sinks, the streamwise direction dimensionless pin spacing has been varied between 1.8 and 3.0, the transverse direction dimensionless pin spacing from 2.5 to 5.0, the dimensionless pin length from 3.0 to 7.0; a reference pin diameter of 2.5 mm has been chosen. For every heat sink configuration, three different frontal air velocities (5, 7.5 and 10 m s^{-1}) have been simulated. A total amount of 108 and 63 simulations has been carried out for the plain finned surfaces and for the pin fin surfaces, respectively. For all the simulations, the flow can be always considered turbulent.

3.1 Heat transfer

Figure 2 shows the effects of the frontal air velocity and of the fin number (i.e. fin pitch) and fin thickness on the heat transfer coefficient for the plain finned surfaces. It can be noticed that the heat

transfer performance increases almost linearly with the frontal air velocity, and also increases when decreasing the fin pitch. Moreover, the heat transfer coefficient increases when increasing the fin thickness; this can be explained considering the increasing of the maximum air velocity when the fin thickness increases at constant fin pitch. On the contrary, the fin height does not affect the heat transfer coefficient. Considering that the surface finned efficiency decreases as the fin height and the air velocity increase and since the heat transfer coefficient α does not depend on fin height, globally, the overall heat transfer coefficient α^* decreases as the fin height increases. Hence, the highest heat transfer coefficient is shown by the finned surface which has the largest fin and the narrowest pitch. Figures 3 shows the effect of the geometrical parameters on the surface finned efficiency. According to the fin theory [7], the finned surface efficiency increases when increasing fin thickness, and when increasing fin pitch, to which a lower heat transfer rate corresponds (see equations (5-6)). The surface finned efficiency also increases when decreasing fin height. An increasing of the specific air mass flow rate leads to a lower efficiency because the heat transfer coefficient increases. Anyway, the values of the finned surface efficiency are always higher than 95%: this is due to the high conductivity of the material of the fins (aluminium alloy) and to the fin geometrical characteristics.

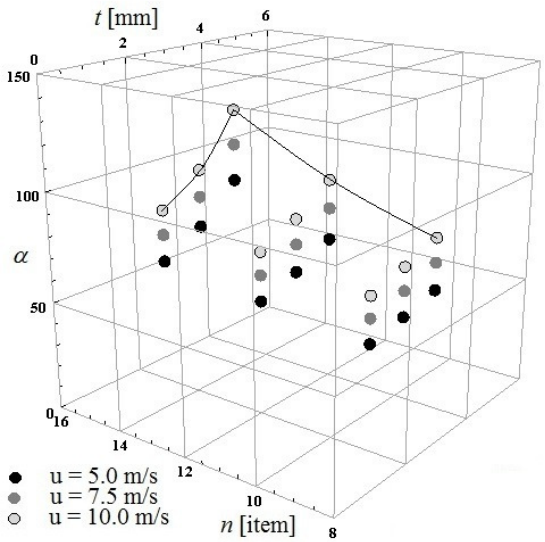

Figure 2. Heat transfer coefficient [W m^{-2} K^{-1}], for the plain finned surfaces, at different air frontal velocities.

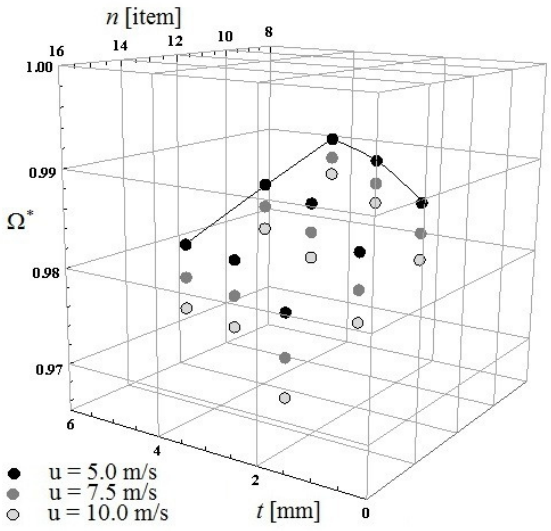

Figure 3. Finned surface efficiency, for the plain finned surfaces, at different air frontal velocities.

Figure 4 shows the effect of the streamwise and transverse direction dimensionless spacing on the heat transfer coefficient for the pin fin surfaces; the pin diameter has been considered as reference dimension. From the numerical simulations it was found that the height of the pin slightly affects the heat transfer performance. Also the contribution of the streamwise direction dimensionless spacing on the heat transfer coefficient is weak, whereas the transverse spacing plays an important role: a decreasing *T*/*d* from 4.8 to 3.2 leads to a 1.33 times higher heat transfer coefficient. The effects of the dimensionless parameters on the finned surface efficiency are shown in figure 5. Ω^* assumes high values for all the simulated geometrical configurations: this is due to the high thermal conductivity of the heat sink material (aluminium alloy) and to their geometrical characteristics. The surface finned efficiency increases when decreasing the *H*/*d* ratio (to which shorter fin heights correspond), when increasing *S*/*d* ratio and when increasing the *T*/*d* ratio (to which a lower heat transfer coefficient corresponds).

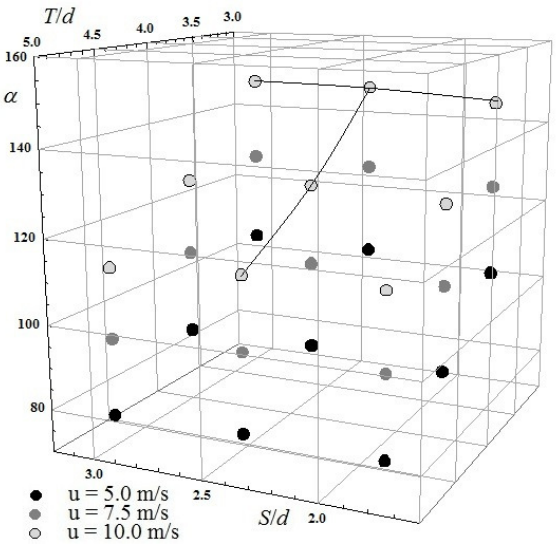

Figure 4. Heat transfer coefficient [W m^{-2} K^{-1}], for the pin fin surfaces, at different air frontal velocities.

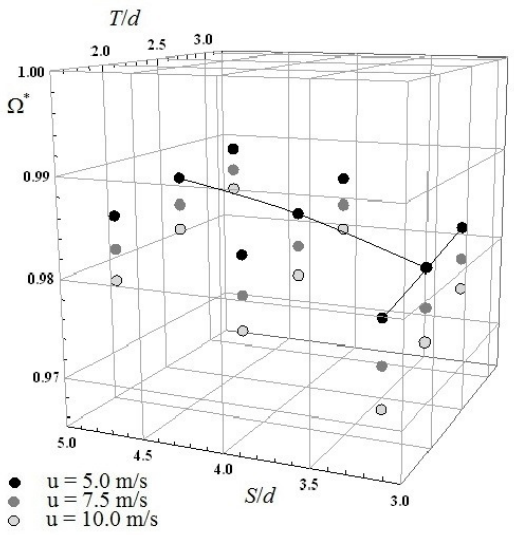

Figure 5. Finned surface efficiency, for the pin fin surfaces, at different air frontal velocities.

The heat transfer coefficient can be expressed using two dimensionless parameters: Nusselt number and Colburn *j*-factor, defined as:

$$\mathrm{Nu} = \frac{\alpha \cdot D_h}{\lambda_{air}} \tag{8}$$

$$\mathrm{j} = \frac{\mathrm{Nu}}{\mathrm{Re} \cdot \mathrm{Pr}^{1/3}} \tag{9}$$

with:

$$\mathrm{Re} = \frac{\rho_{air} \cdot u_{\max} \cdot L_c}{\mu_{air}} \tag{10}$$

where λ_{air}, ρ_{air}, μ_{air} and Pr are the thermal conductivity, density, dynamic viscosity and the Prandtl number of the air calculated at the mean value of temperature and pressure, u_{max} is the maximum air velocity referred to the minimum cross sectional area, L_c is the characteristic length, which is the hydraulic diameter D_h for the plain finned surface and the pin diameter d for the pin fin surfaces.

The numerical thermal results have been compared against empirical correlations from the open literature. For the plain finned surfaces, the numerical values of Nusselt number have been compared with those predicted by the correlations proposed by Polley and Abu-Khader [10] and by Wu et al. [11]. The correlations by Polley and Abu-Khader [10] tends to underestimate the thermal behavior of the simulated plain finned surfaces; the relative, absolute and standard deviations are: -11.3%, 11.5% and 5.4%. The correlation of Wu et al. [11] shows a relative, absolute and standard deviations on the Nusselts number of: -11.3%, 14.5% and 13.7%. For the pin fin heat sinks, the correlation of Short et al. [5] has been selected and it tends to underestimate the numerical values: for the Colburn j-factor, the relative deviation is -19.2%, the absolute deviation 20.2% and the standard deviation 12.3%.

Starting from the numerical results, two new correlations for the prediction of the thermal behavior of plain fin and pin fin heat sink have been developed and proposed. The thermal performance can be expressed in terms of Colburn j-factor with the following two equations, for plain finned surfaces (Re = 2700 ÷ 10100, Pr = 0.7) and for pin fin surfaces (Re = 1000 ÷ 4200, Pr = 0.7), respectively:

$$\mathrm{j} = 0.233 \cdot \left(\frac{t}{H}\right)^{-0.208} \cdot \left(\frac{p}{H}\right)^{0.192} \cdot \mathrm{Re}^{-0.48} \tag{11}$$

$$j = 0.327 \cdot \left(\frac{S}{d}\right)^{0.037} \cdot \left(\frac{T}{d}\right)^{-0.397} \cdot \left(\frac{H}{d}\right)^{0.201} \cdot \mathrm{Re}^{-0.45} \quad (12)$$

These two correlations result accurate: for the plain fin surfaces, the numerical j-Colburn factors are estimated with a relative deviation of -0.4%, an absolute deviation of 4.3% and a standard deviation of 5.3%, with almost all of the points within ±10%, and for the pin fin surfaces with a relative deviation of 0.1%, an absolute deviation of 3.3%, a standard deviation of 3.7% and with all the points within ±8%.

3.2 Pressure drop

The effect of the fin number and fin thickness on the pressure drop behavior for the plain finned surfaces is shown in figure 6. The numerical pressure drop exhibits a parabolic dependence on the fluid velocity. As expected, the pressure drop increases when increasing fin number (i.e. fin pitch) and fin thickness; on the contrary, the fin height slightly affects the fluid dynamic behavior: pressure drops slightly increase when decreasing fin height.

Figure 7 shows the effects of the geometrical parameters on the fluid flow performance of the pin fin surfaces. The decreasing of the dimensionless transverse spacing *T*/*d* leads to higher pressure drop: in the simulated range of geometrical parameters, the pressure drops double. In addition, unlike for what highlighted for the heat transfer coefficient, also the streamwise dimensionless spacing affects the pressure drops: they increase when *S*/*d* decreases. *H*/*d* slightly affects the hydraulic behavior.

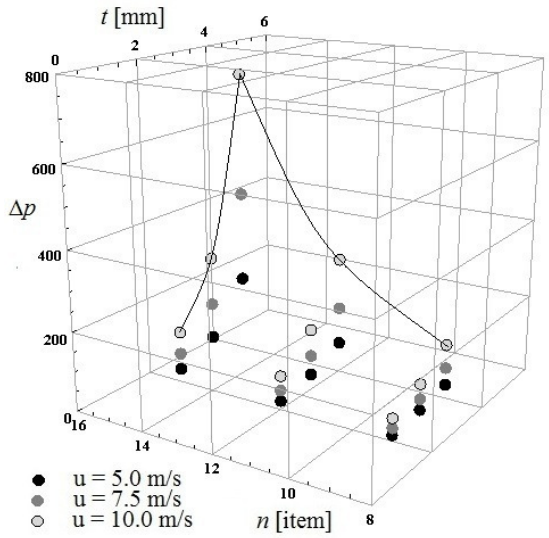

Figure 6. Pressure drop [Pa], for the plain fin surfaces, at different air frontal velocities.

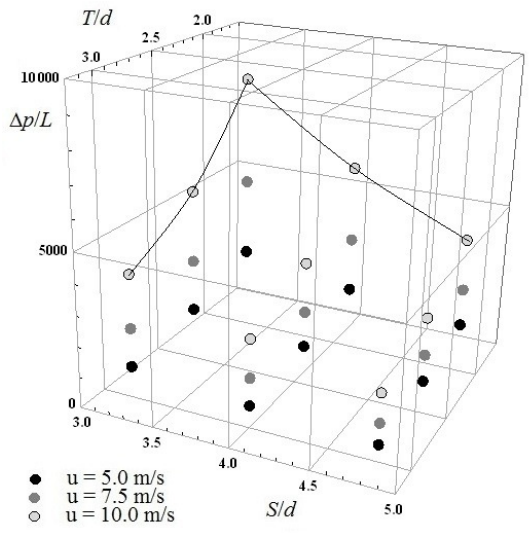

Figure 7. Pressure gradient [Pa m^{-1}], for the pin fin surfaces, at different air frontal velocities.

The pressure drops for the plain fin surfaces can be considered as the sum of three contributions: contraction and expansion losses at the inlet and at the outlet of the extended surfaces, and core friction losses. Thus, the total pressure drop can be expressed as:

$$\Delta p_{tot} = \Delta p_c + \Delta p_e + \Delta p = \frac{1}{2}\rho \cdot u^2{}_{\max} \cdot \left[K_c + K_e + 4 \cdot f \cdot \frac{L}{D_h}\right] \quad (13)$$

where L is the length of the finned surface and K_c and K_e are the contraction and expansion coefficients, as suggested by Kays and London [12] for the turbulent flow regime, while f is the core friction factor. For the pin fin surfaces, the apparent friction factor is commonly used to describe the pressure drop:

$$f_{app} = \frac{\Delta p_{tot} \cdot L_c}{2 \cdot \rho_{air} \cdot l \cdot u^2{}_{\max}} \tag{14}$$

For the plain fin surfaces, the correlation of Polley and Abu-Khader [10] tends to underestimate the numerical core friction factor with a relative, absolute and standard deviation of: -33.6%, 33.6% and 5.7%, respectively. The correlation of Wu et al. [11] results more accurate for the prediction of the core friction factor, with a relative deviation of -8.2%, an absolute deviation of 8.3% and a standard deviation of 6.3%.

For the pin fin surfaces, the correlation of Short et al. [4] for the estimation of the apparent friction factor shows a relative, absolute and standard deviation of: -26.9%, 26.9% and 4.4%, respectively.

The numerical results have permitted to develop two new correlations for the estimation of the core friction factor for the plain surfaces (Re = 2700 ÷ 10100, Pr = 0.7) and of the apparent friction factor for the pin surfaces (Re = 1000 ÷ 4200, Pr = 0.7):

$$f = 0.029 \cdot \left(\frac{t}{H}\right)^{0.034} \cdot \left(\frac{p}{H}\right)^{-0.169} \cdot \mathrm{Re}^{-0.09} \tag{15}$$

$$f_{app} = 0.227 \cdot \left(\frac{S}{d}\right)^{-1.307} \cdot \left(\frac{T}{d}\right)^{-0.692} \cdot \left(\frac{H}{d}\right)^{0.107} \cdot \mathrm{Re}^{-0.04} \tag{16}$$

The core friction factors of the plain surfaces are predicted with a relative, absolute and standard deviation of: 0.2%, 2.9% and 3.4%, respectively, whereas the apparent friction factors of the pin fin surfaces with a relative, absolute and standard deviation of: 0.2%, 4.9% and 6.1%, respectively.

4. Conclusions

This paper reports a numerical study on air forced convection in turbulent flow through rectangular plain finned surfaces and pin fin surfaces. For each type of surface, the effect of the geometrical parameters on the thermal and fluid flow performance have been analyzed using the CFD software COMSOL Multiphysics [6] with the standard *k*-ε model. The numerical tool has been validated with the experimental heat transfer coefficients and pressure drops measured during air forced convection through a reference finned surface and the suitability of the numerical tool have been confirmed.

For the plain fin surfaces, the models of Polley and Abu-Khader [10] and of Wu et al. [11] have been selected and checked, whereas, for the pin fin surfaces, the models of Short et al. [4-5]. Moreover, four new correlations for the estimation of thermal and hydraulic performance of plain finned and pin fin surfaces are proposed and validated. These new models can be used to design the most suitable heat sink configuration for a given electronic cooling application.

5. References

[1] Kandlikar S G, Garimella S, Colin S and King M R 1992 *Heat Transfer and Fluid Flow in Minichannels and Microchannels* (Oxford: Elsevier) chapter 3
[2] Mancin S, Zilio C, Cavallini A and Rossetto L 2010 *Int. J. Heat Mass Transf.* **53** 4976-84
[3] Mancin S, Zilio C, Cavallini A and Rossetto L 2010 *Int. J. Heat Mass Transf.* **53** 3121-30
[4] Short B E, Raad P E and Price D C 2002 *J. Thermophys. Heat Transf.* **16**(3) 389-396
[5] Short B E, Raad P E and Price D C 2002 *J. Thermophys. Heat Transf.* **16**(3) 397-403
[6] COMSOL Multhiphysics 3.5a 2008
[7] Incropera F P and DeWitt D P 2008 *Fundamentals of Heat and Mass Transfer* (NY: Wiley)
[8] Cavallini A, Mancin S, Rossetto L and Zilio C 2008 *Proc. 8th Gustav Lorentzen Conference on Natural Working Fluids (Copenhagen, Denmark, 7-10 September 2008)*
[9] Diani A, Mancin S, Zilio C and Rossetto L 2011 *XXIX National Heat Transfer Conference (Turin, Italy, 20-22 June 2011)*
[10] Polley G T and Abu-Khader M M 2005 *Heat Transf. Eng.* **26**(9) 15-21
[11] Wu H H, Hsiao Y Y, Huang H S, Tang P H and Chen S L (2011) *Appl. Therm. Eng.* **31** 984-92
[12] Kays W M and London A L 1984 *Compact Heat Exchanger* (NY: Mc Graw-Hill)